Received: 22 June 2023 | Revised: 29 February 2024 | Accepted: 10 April 2024

DOI: 10.1002/joc.8468

International Journal of Climatology | RMetS

RESEARCH ARTICLE

Spatiotemporal variability of the rainy season in the Yucatan Peninsula

David Romero[1] | **Eric J. Alfaro**[2]

[1]Escuela Nacional de Estudios Superiores, Unidad Mérida, Universidad Nacional Autónoma de México, Ucu, Mexico

[2]Escuela de Física, Centro de Investigaciones Geofísicas y Centro de Investigación en Ciencias del Mar y Limnología, Ciudad Universitaria Rodrigo Facio, Universidad de Costa Rica, San Jose, Costa Rica

Correspondence
David Romero, Escuela Nacional de Estudios Superiores, Unidad Mérida, Universidad Nacional Autónoma de México, Carretera Merida-Tetiz, km 4, 97357 Ucu, Yucatan, Mexico.
Email: dromero@enesmerida.unam.mx

Funding information
Universidad de Costa Rica; Universidad Nacional Autónoma de México, Grant/Award Number: IA302220

Abstract

The rainfall regime is a critical factor in the Yucatan Peninsula, as the spatial and multiannual variability of rainfall is a major concern, particularly for crops. Variability in the rainy season was examined considering the onset and demise of the annual rainy season, the total rain volume, the rainfall season duration and the intense precipitation events recorded in meteorological stations (1978–2020). We analysed individual time series and calculated the long-term trend. Additionally, we explored the relationship between each summer rainfall characteristic and several oceanographic indices using multivariate techniques. We also developed a Trans-Isthmic Index from the relationship between the El Niño–Southern Oscillation and the Atlantic Multidecadal Oscillation. This index allows for determining the effect of the overall influence of the ocean on climate. The timeseries analysis revealed a high interannual variability and long-term positive trends concerning the duration of the rainy season with earlier onset and later demise, and the total rainfall volume and also a positive trend for the occurrence of heavy precipitation suggesting a shift in intra-annual patterns. Spatially, the analysis revealed clusters of stations with a similar variation, probably related to the AMO, NIÑO3.4 or TII indices. The spatial pattern was confirmed by analysing CHIRPS gridded precipitation data. Our results show that wetter conditions are associated with lower temperatures in the equatorial Pacific and warmer conditions in the Atlantic.

KEYWORDS
AMO, climate variability, ENSO, precipitation

1 | INTRODUCTION

The Yucatan Peninsula (YP), Mexico, has a tropical, warm and mainly subhumid climate. Virtually the entire area (97.2%) belongs to the Aw and Ax′(w) climate types (0, 1 or 2) of Köppen's climate classification modified for Mexico by García (García, 2004), while the northwestern coastal strip (1.4%) is arid and semi-arid with a BS climate type (0 and 1), and the Campeche zone bordering Tabasco, as well as Cozumel Island (1.4%) have a more humid climate (Am) (Vidal, 2005). The rainfall regime in the area spans from mid-spring to mid-autumn (from

May to October), almost exclusively in the west of the peninsula (Aw climate); it is more homogeneous in the east, with slight intra-annual variations (Vidal, 2005) (Ax′ (w) climate), while the trade winds, constantly flowing the rest of the year, bring scarce rainfall associated with convective rain due to the flat relief and the leeward position of the peninsula relative to the trade winds (McGregor & Nieuwolt, 1998).

In the YP, the rural population, which is relatively abundant—approximately 792,138 inhabitants in 2020, according to the National Institute of Statistics and Geography (INEGI, 2021)—depends on seasonal agriculture, mainly corn, except in the arid climate zone. The Agrifood and Fish Information Service (SIAP) reported 396,383 ha of rainfed crops on the peninsula in 2020, of which 325,845 ha correspond to maize grown in spring–summer (SIAP, 2021). This sector is adapted to drought but is subject to significant fluctuations or a more general nature, likely associated with climate change. Yucatan farmers report an increase in the incidence of intense drought events linked to a delayed onset of the rainy season, which affects crops. In addition, drought substantially impacts livestock; pigs and bovine livestock, which are highly water-demanding, are gaining increasing importance in the regional economy.

The rainy season in the YP is characterized by complex spatiotemporal variations that influence the onset, demise, duration and volume of rainfall during this season. Understanding these variations is essential for planning in various sectors, including agriculture, water and natural resource management.

Recent studies have highlighted the importance of understanding the spatiotemporal variation of the rainy season in the Yucatan Peninsula. For the south of the YP, Mardero et al. (2020) detected no changes in the onset of the rainy season over the past few decades. However, these authors recorded an increased frequency of intense rainfall events, leading to higher volumes of rainfall received. Similarly, Mardero et al. (2018) noted a high spatial variability in the average amount of rainfall across the three states located in the YP (Yucatán, Chiapas and Campeche), which has major implications for agriculture and natural resource management. These studies highlight the need for a detailed analysis of the spatiotemporal variations of the rainy season in this region, which is the objective of the present study.

Understanding the spatiotemporal variations of the rainy season in tropical areas is essential to develop effective adaptation strategies and policies to mitigate the potential impacts of climate change (Dunning et al., 2018). An improved understanding of the spatiotemporal variability of the rainy season can help farmers and water managers optimize irrigation strategies and water allocation schemes to improve water use efficiency and agricultural productivity in the region (Mardero et al., 2018).

It is important to document the variability of summer rainfall in the YP with daily and monthly data because they reflect different time scales that are useful for understanding rainfall patterns and their impacts on the region. According to Durán-Quesada et al. (2017), the main sources of moisture from the surrounding oceans are the tropical North Atlantic Ocean and the Caribbean Sea.

Daily data provide a more detailed and accurate picture of rainfall patterns and their variability, allowing a better understanding of how rainfall affects the region on a daily basis. This level of detail is useful to identify short-term fluctuations in rainfall and to explore how these fluctuations impact the environment, agriculture and society (Romero et al., 2017, 2020). Daily data also help identify extreme rainfall events, such as heavy storms or prolonged droughts that can significantly impact the region. Furthermore, the YP is a region with mostly flat terrain, and daily data can help identify spatial variability in rainfall that may go unnoticed with monthly data. Understanding daily patterns of data changes is particularly important for agriculture, where crops are often sensitive to variations in daily rainfall. The onset, demise of the rainy season and the number of days with heavy rainfall can be calculated using monthly data.

On the other hand, monthly data provide a broader view of the rainfall regime over a longer period. These data allow for the identification of seasonal and annual rainfall patterns, which can support predictions of future changes in rainfall and the development of long-term strategies to manage water resources and mitigate the impacts of extreme weather events. Monthly data are also useful for identifying long-term trends in rainfall, such as changes in precipitation patterns due to climate change. Meanwhile, monthly cumulative data are adequate for investigating seasonal aspects (Mardero et al., 2020).

Given its location on the Central American isthmus and its flat relief, the YP shows a heterogeneous rainy season. It may be influenced by atmospheric and marine circulations in the Atlantic and Pacific oceans. The Atlantic Multidecadal Oscillation (AMO) and El Niño–Southern Oscillation (ENSO) are two major climate phenomena that can interact and influence each other (Levine et al., 2017), affecting global climate variability. The AMO is a natural climate cycle in the North Atlantic basin characterized by changes in sea surface temperature (SST) over decades. ENSO is a coupled ocean–atmosphere phenomenon in the tropical Pacific Ocean that shows interannual variations in SST and atmospheric pressure. We did not include the Pacific Decadal Oscillation in the study because this relationship, although related to local climatic conditions (Andrade-

Velázquez et al., 2021), depends on ENSO (Pavia et al., 2006), with which it is strongly correlated (Kwon et al., 2013), and ENSO has a strong relationship with regional climate (Rodríguez Morales et al., 2023).

The interaction between AMO and ENSO has been the subject of several studies in recent years, as understanding their interaction is crucial to predicting and mitigating the impacts of climate variability. A study found that the AMO phase can influence the strength and duration of El Niño and La Niña events, with a positive AMO phase frequently associated with more intense El Niño and weaker La Niña events (Wang, 2019). In Central America, Maldonado et al. (2016, 2017) have suggested that SST is higher in the Atlantic Ocean and lower in the eastern equatorial Pacific; the rainy season in Central America tends to be wetter, while it is drier under opposite ocean conditions, particularly, but not exclusively, on the Pacific slope. Another study suggested that the interaction between AMO and ENSO may explain some of the changes in rainfall patterns observed in the Amazon basin (García-García & Ummenhofer, 2015; Toshie Kayano & Buscioli, 2014) and Florida (Abiy et al., 2019; Goly & Teegavarapu, 2014). In a recent study focused on coastal stations and summer rains, Rodríguez Morales et al. (2023) found that rain is more abundant in the northern region of the Yucatan Peninsula during the AMO warm phase. On the west coast of the Yucatan Peninsula, they observed a few points that exhibited opposite behaviour, with significant differences between them. The northeastern zone recorded higher precipitation during La Niña and a negative AMO phase.

The present work aims to provide an overview of the spatiotemporal variation of the rainy season in the Yucatan Peninsula based on recent research and data analysis. We will examine the onset and demise dates of the rainy season, its duration, the amount of rainfall during this season, and the days with heavy precipitation events to determine the presence of temporal trends and the spatial influence of oceanographic oscillations. We hypothesize that rainfall variability during the rainy season at the meteorological station level depends on the variability in the oceans surrounding the YP by modulating aspects such as heavy rainy days, onset, demise and accumulated rainfall.

2 | DATA AND METHODS

2.1 | Data

2.1.1 | Data from meteorological stations

Mexico's National Meteorological Service (SMN, in Spanish) maintains the national climatological database for Mexico, integrated into the Climate Computing project (CliCom). This project consists of a quality-controlled data set using Climate Computing software developed by the United Nations Organization and incorporated into the data set by Dunn et al. (2020) (Sáenz et al., 2023). Observations at each of the 5459 meteorological stations in the country are recorded daily at 0800 LST (local standard time). The daily data represent the previous 24 h, ending at 0800 LST the next day (1400 UTC, 1300 by applying daylight-saving time). The CliCom data series spans from 1902 to 2020; however, the period covered by each station varies from 30 days to 118 years, with a median of 38 years, including gaps in the time series; there are major data lags in the time series before the mid-1970s. The data included are daily and monthly values of observed minimum and maximum temperature (°C), precipitation (mm), evaporation (mm), occurrence of electrical storms, hail, fog, frost, and two cloudiness levels.

The variability of summer rainfall on the Yucatan Peninsula is critical in Group A climate zones, as it supplies water for rainfed agriculture. Consequently, considering low lag rates and homogeneous time series until 2020, we selected 109 meteorological stations on the Yucatan Peninsula belonging to Group A climates for the study; data recorded before 1978 were excluded.

2.1.2 | Gridded data

CHIRPS (Climate Hazards Group InfraRed Precipitation with Station data) is a gridded precipitation data set (Funk et al., 2015). The data, derived from satellite data and ground-station measurements, allow for more accurate and detailed information about precipitation patterns. The CHIRPS data set is also available at different temporal resolutions (daily to monthly) from 1981 to the present.

The CHIRPS data set provides gridded precipitation data at a spatial resolution of 0.05°, corresponding to approximately 5.5 km at the equator. This high resolution allows detailed analyses of precipitation patterns at the local level, which is particularly important for studies on climate variability and its impact on local communities. Indeed, CHIRPS provides precipitation estimates in regions lacking ground stations. These estimates are particularly useful for studying precipitation in remote regions, such as the south of the Yucatan Peninsula. An advantage of the data set is the availability of near-present data, which is helpful for more robust statistical timeseries analyses and updated studies on climate variability and climate change. Furthermore, Centella-Artola

et al. (2020) evaluated different gridded rainfall databases for the Caribbean region against gauge station data that further validated the CHIRPS data set. Their comparison methods were the modified efficiency index of Kling-Gupta (KGE′) (Kling et al., 2012) and the standardized precipitation index (SPI) at 3, 6 and 12 months (McKee et al., 1993). Other authors have also validated the use of CHIRPS for Central America (Stewart et al., 2022). In the present study, we also applied KGE′ to compare gridded data for the 109 stations; the mean KGE′ value was 0.84 ± 0.06. This study used monthly rainfall data for the whole database period.

2.2 | Data-filling technique

The time series of daily meteorological data from the 109 stations contains information gaps. To fill these gaps, daily rainfall values in the study area were interpolated from existing data using the Inverse Distance Weighted (IDW) method; values were interpolated for locations corresponding to stations with missing data. To determine the optimal parameters (inverse distance power [IDP] for weighting and number of neighbours) for use in IDW, we randomly extracted 1000 values from the database. These values were estimated through interpolations using powers ranging from 0 to 5 and varying the number of neighbours from 1 to 10. Subsequently, the determination coefficient (r^2) between the observed and the estimated data series was calculated. The mean standard error (MSE) was computed, and the best validation parameters were used to fill in the missing values in the entire database. The best combination of parameters was IDP = 3 and neighbours = 2, giving $r^2 = 0.998$ and MSE = 0.48.

2.3 | Rainy season onset and demise estimation

After filling in the daily records for the 109 stations selected, we smoothed every record using a triangular 31-day moving average, according to Soley (1994), to reduce the high daily variability. The rainy season onset date was calculated for every year and station; when it occurred after April 1, the onset date is defined as the first of a sequence of 10 consecutive days in the smoothed data with rain above the 5 mm threshold and at least 0.1 mm in each of the following consecutive 5 days, using the methodology suggested by Gramzow and Henry (1972) and Enfield and Alfaro (1999) for tropical regions. No note, the period before April 1 corresponds to the dry season, and the rains associated with cool fronts during this period should not be assimilated with the more convective precipitation typical of the rainy season. With this technique, we obtained 109 timeseries records of the onset date, each spanning 41 years. The demise of the rainy season was calculated similarly but with smoothed daily records from November 30 to the beginning of the following year. We reviewed the records from April to November because this is the season with more convective activity according to the annual precipitation cycle in the region (Amador, 2008; Magaña et al., 1999) and to mitigate the potential influence of late or early cold-front intrusions with the associated stratiform rain (Magaña & Vázquez, 2000). Onset dates later than June 30 and demise dates earlier than September 1 were excluded because of the potential confusion with the start and end of the mid-summer drought (García-Franco et al., 2023).

Finally, maps showing ranges of the median of each component of the rainy season for the entire domain were elaborated.

2.4 | Data analysis

We computed long-term trend analyses for the components of the rainy season (onset, demise, duration, rainy season accumulated precipitation [RSAP] and the number of days with intense rainfall). We first calculated the number of days with rainfall ≥10 mm (dR10) and ≥20 mm (dR20) between May and October as modified Climdex indices (Karl et al., 1999; Peterson et al., 2001). We then constructed annual boxplots that included all stations, applying a linear regression model (Wilks, 2019) to the annual values.

In addition, we conducted a Spearman's rank-order correlation between annual timeseries data for each station and the mean values for the rainy season of the climate indices that may influence precipitation at the regional level: Atlantic Multidecadal Oscillation (AMO) (Enfield et al., 2001) and NIÑO3.4 (Trenberth & Stepaniak, 2001). The NOAA Climate Prediction Center computes the indices and shares them at https://psl.noaa.gov/data/climateindices/list/. The Spearman correlation considered a p-value <0.05 as the statistical significance threshold. Both indices yielded significant results.

To evaluate the effects of the interrelation between Atlantic and Pacific Ocean temperatures on rainfall in the YP, a Trans-Isthmic Index (TII) was calculated using the following Equation (1),

$$\mathrm{TII}_{ij} = \frac{\mathrm{NIÑO3.4}_{ij} - \overline{\mathrm{NIÑO3.4}_i}}{S_{\mathrm{NIÑO3.4}_i}} - \frac{\mathrm{AMO}_{ij} - \overline{\mathrm{AMO}_i}}{S_{\mathrm{AMO}_i}}, \quad (1)$$

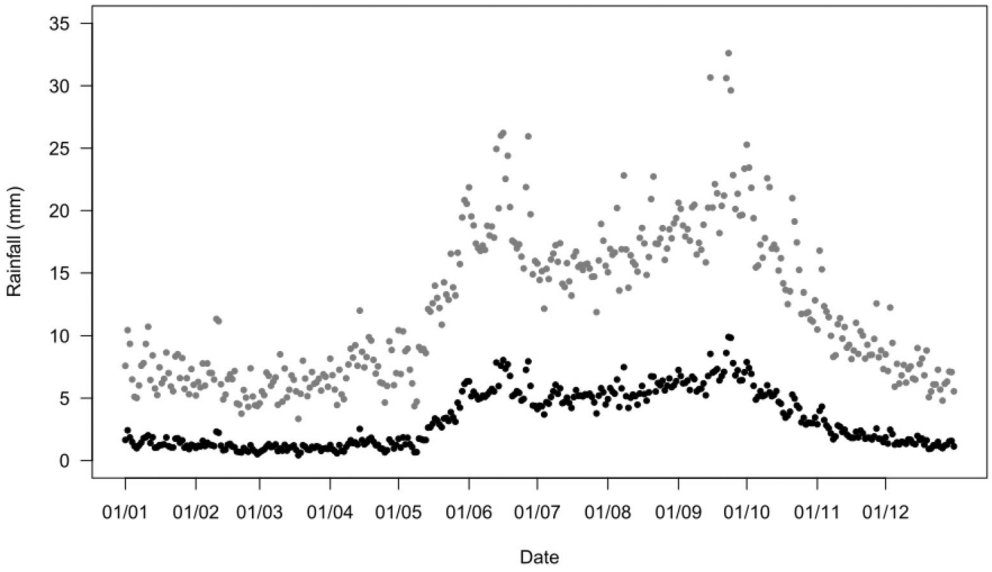

FIGURE 1 Daily rainfall in the 109 meteorological stations located in the study area. Black dots represent mean values; grey dots, means + one standard deviation.

where TII_{ij}, $NIÑO3.4_{ij}$ and AMO_{ij} are, respectively, the Trans-Isthmic Index, the NIÑO3.4 index, and the AMO index for month i and year j. $\overline{NIÑO3.4_i}$, $\overline{AMO_i}$, $S_{NIÑO3.4_i}$ and S_{AMO_i} are the mean and the standard deviation values of, respectively, the NIÑO3.4 index, and the AMO index for month i during the baseline period. The years used for climatology, that is, the computation of the mean and standard deviation of input indices, were 1971–2000 as a three-decade period is commonly used for this purpose (Hoerling et al., 2010; Penland & Matrosova, 1998; WMO, 2017). This particular one is used for various climate indices (Enfield et al., 1999; Wang & Enfield, 2001). The selection of a baseline period for calculating the TII may influence the index results, as different baseline periods could result in different interpretations of the interrelation between ocean temperatures and rainfall.

Subsequently, the TII was integrated into the multivariate analysis. It is important to note that this study used an unsmoothed AMO version that incorporates an interannual variability greater than the decadal variability. Consequently, the baseline selection for TII computing should not influence the multivariate analysis.

To improve the evaluation of the local impact of the different indices, a linear regression was also applied to the rainy-season rainfall volume for each pixel of the CHIRPS gridded data. This spatial analysis identified the index with the greatest relationship with rainy-season cumulative data and the type of relationship (positive or negative). Finally, the use of CHIRPS data was validated by comparing the signs of the Spearman correlation between station RSAP values and climate indices with the linear regression estimates from CHIRPS.

3 | RESULTS

3.1 | Characterization of the rainy season

The annual cycle of mean daily precipitation for the stations included in this work is shown in Figure 1. This cycle shows a well-defined bimodal rainfall distribution pattern with peaks in June and September, separated by a relative minimum in July–August—a common precipitation feature in Mesoamerica called the Midsummer Drought (García-Franco et al., 2023; Perdigón-Morales et al., 2018). Rains tend to start with a shift in the inflection point around May 15, with increased precipitation (Figure 1). By contrast, the demise of the rainy season is not well defined; it occurs around November 1, with a gentle transition due to the occurrence of early cold fronts (Zárate-Hernández, 2013). The annual volume is approximately 1204.8 mm, with a high interannual variation. Martinez et al. (2019) proposed a scheme to show the interactions of the main climatological features in Mesoamerica throughout the seasonal cycle. The Intra-Americas Sea strongly influences the YP, surrounded by the Gulf of Mexico (west) and the Caribbean Sea (east).

The results in Figure 2 show a variation under the more arid conditions of the northwest YP, with later onset dates, earlier demise dates and, therefore, shorter duration. Additionally, the May–October period shows lower cumulative rainfall and fewer days of heavy rains. According to the methodology, the rainy season begins between May 21 and June 30 (Figure 2a) and ends between September 28 and November 14 (Figure 2b). In November, despite rains that are part of the summer

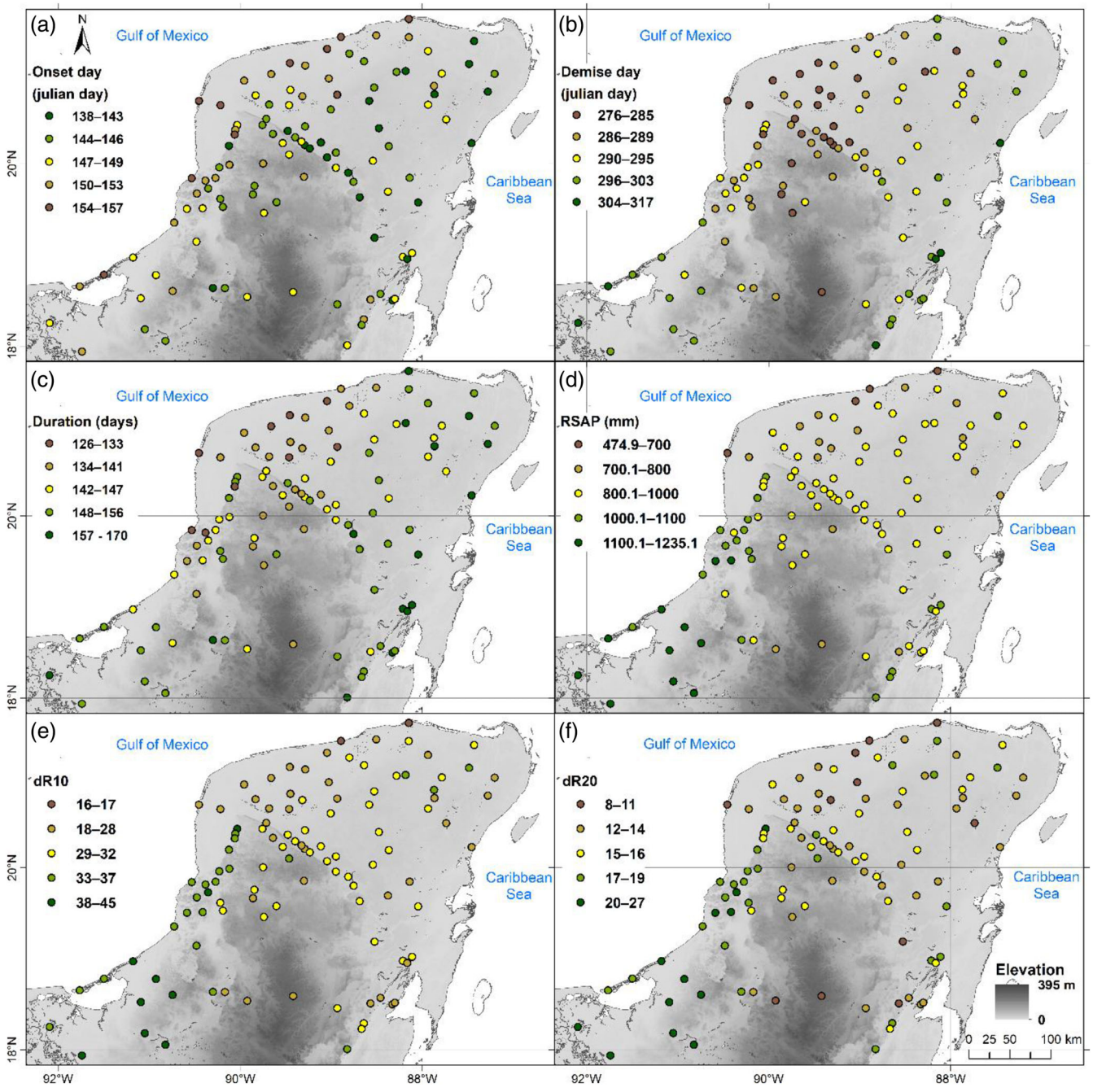

FIGURE 2 Median rainy season values by station of (a) onset date, (b) demise date, (c) duration calculated as the demise date minus the onset date, (d) cumulative precipitation, (e) dR10 and (f) dR20. [Colour figure can be viewed at wileyonlinelibrary.com]

season, the cumulative volume of rainfall is low, as shown in Figure 1, probably influenced by non-convective rains such as those associated with early cold fronts, locally known as *Nortes* (Magaña & Vázquez, 2000). Consequently, the summer rainfall period lasts 126–170 days (i.e., 4–6 months) (Figure 2c).

In the south of the YP, the rainy season tends to last longer in the southeastern zone. On the other hand, cumulative rainfall is higher in the western plain. The central area lacks gauge stations, but the few that operate indicate a shorter season with less cumulative rainfall (Figure 2c,d).

This spatial pattern is confirmed by the distribution of median dR10 and dR20 values (Figure 2e,f). Both variables have similar spatial patterns, showing peaks in the southwest (up to 45 and 27 days, respectively) and low values similar recorded for the northern dry zone (≤17 and ≤11 days, respectively).

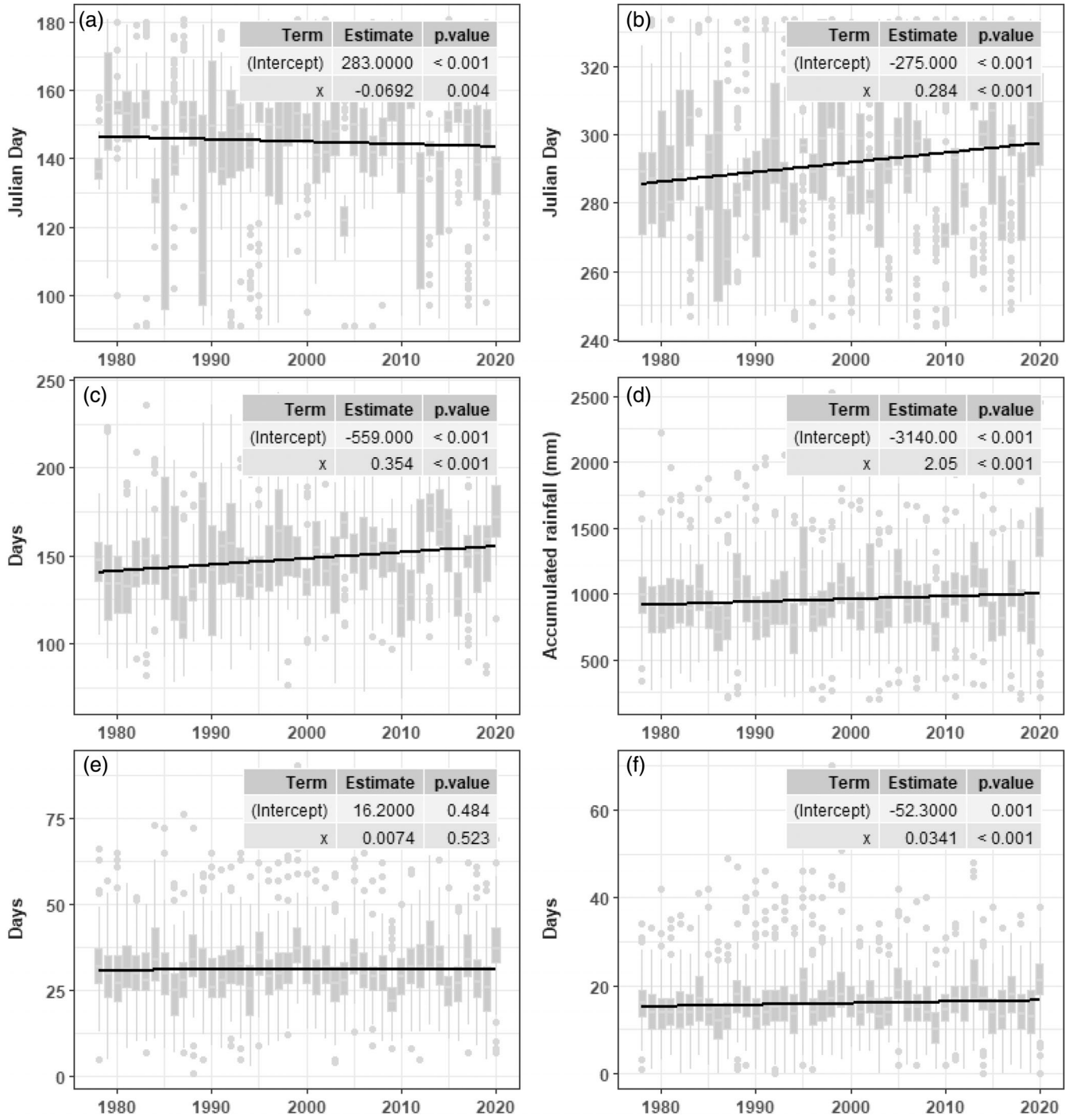

FIGURE 3 Annual rainy season boxplot of (a) onset date, (b) demise date, (c) duration, (d) cumulative precipitation, (e) dR10 and (f) dR20. Whiskers represent ±1.5 IQR; solid black lines represent the trends.

3.2 | Temporal trends for rainy season components at gauge stations

For the study area, the long-term trend for the onset date of the rainy season or the RSAP was negative and the RSAP was positive ($p < 0.05$) (Figure 3a,d), with a high spatiotemporal variation. This finding is consistent with Mardero et al. (2018, 2020), who did not find a reduction in rainfall volume in the region. This is a central aspect to consider when perception studies on the population are conducted, given that the press extensively broadcasts these variables due to their marked impact on agriculture (Martins, 2021). We also found significant positive trends for the rainy season demise date, duration and dR20 ($p < 0.05$) (Figure 3b,c,f), but nonsignificant for dR10 (Figure 3e). This finding is critical because when studying

TABLE 1 Percentage of stations with a significant Spearman's rank-order correlation, considering the climate indices.

	Onset (%)	Demise (%)	Duration (%)	dR10 (%)	dR20 (%)	RSAP (%)
AMO+	3.7	11.0	6.4	13.8	17.4	17.4
AMO−	0.0	0.0	0.0	3.7	3.7	2.8
NIÑO3.4+	0.9	2.8	5.5	0.0	0.0	0.0
NIÑO3.4−	1.8	3.7	0.0	26.6	23.9	33.9
TII+	0.0	0.0	0.9	1.8	0.0	0.0
TII−	1.8	4.6	0.9	26.6	26.6	33.9

Note: The + or − sign refers to the sign of the correlation. The total number of stations is 109.

climate change, one must consider changes in the average conditions as well as in variability. In other words, our results suggest statistically significant evidence of change in the amount of rain; also, the rainfall pattern has changed, with more episodes of heavier rain, fewer episodes of light, and longer rainy seasons (IPCC, 2022), which may lead to an increased risk of floods and a less effective use of rainfall by vegetation, particularly rainfed crops. Furthermore, there is a large spatial dispersion around the average conditions (Figure 3); this indicates that management measures that could be applied for a specific sector, such as agriculture, may differ in geographically close areas due to the local climatic conditions. This is particularly the case in the YP due to the lack of orographic convection (Romero et al., 2020) and is a critical aspect to consider for studies on planning and adaptation to climate change (IPCC, 2022).

3.3 | Determination of the oceanic influence on stations

The influence of climate indices on the onset date, demise date and duration of the summer rainy season is not clearly defined. Indeed, only slightly more than 5% of the stations exhibited a significant Spearman correlation for AMO+ with onset date (11%) and duration (6.4%) (Table 1). The impact of the ENSO appears marginal, with few stations showing a significant correlation and with positive and negative relationships in similar proportions. Local mesoscale factors associated with convective rain apparently control the variability in onset and demise dates.

Conversely, for dR10, dR20 and RSAP, the relationships between time series and indices were more prevalent (Table 1), predominantly associated with NIÑO3.4− and TII−.

The AMO, NIÑO3.4 and TII correlation maps show strong relationships with RSAP and dR20 (Figure 4). As we considered a 95% significance level, we did not build maps for the other precipitation variables since very few stations met this statistical significance threshold.

The spatial variation of the correlations with RSAP shows the importance of the TII, with 33.9% of the stations with significant values showing a negative correlation between RSAP and TII (Figure 4a and Table 1). This suggests that RSAP tends to be higher when the eastern equatorial Pacific is relatively cold and the Atlantic is relatively warm; when these ocean conditions are reversed, RSAP tends to be lower. These strong relationships were observed primarily in the northwest of the YP. The influence of NIÑO3.4 is also remarkable in 33.9% of the stations, most of which are located in the mid-eastern and western limits of the study area, associated with the dominance of NIÑO3.4. Additionally, despite being dominant in fewer stations, mainly in the northeast and around the Bay of Campeche in the southwest, through strong positive correlations, AMO+ showed a significant correlation with RSAP in 17.4% of the stations (Table 1).

In the case of dR20 (Figure 4b), a similar positive relationship with the AMO is observed in 17.4% of the stations (Table 1); note that the spatial distribution of the stations where this index dominates does not correspond to the pattern defined by the previous ones; instead, these stations are distributed throughout the YP (Figure 4b). This is consistent with the results of the TII because these stations also yielded several negative correlations (26.6%). The influence of ENSO, regardless of its interactions with the Atlantic, evidenced by the relationship with NIÑO3.4, is lower for dR20 with 23.9% than for dR10 with 26.6% of the stations. The spatial results for dR10 and dR20 were very similar; therefore, this work shows only the dR20 results, with the dR10 results detailed in Data S1, Supporting Information. In general, the spatial distribution of the dominance indices for dR20 and dR10 (Figure S1) is poorly defined relative to RSAP, for which spatial clusters are observed. Regarding the percentage of stations with significant relationships between dR10 and the indices, the values were similar to those obtained for RSAP (Table 1).

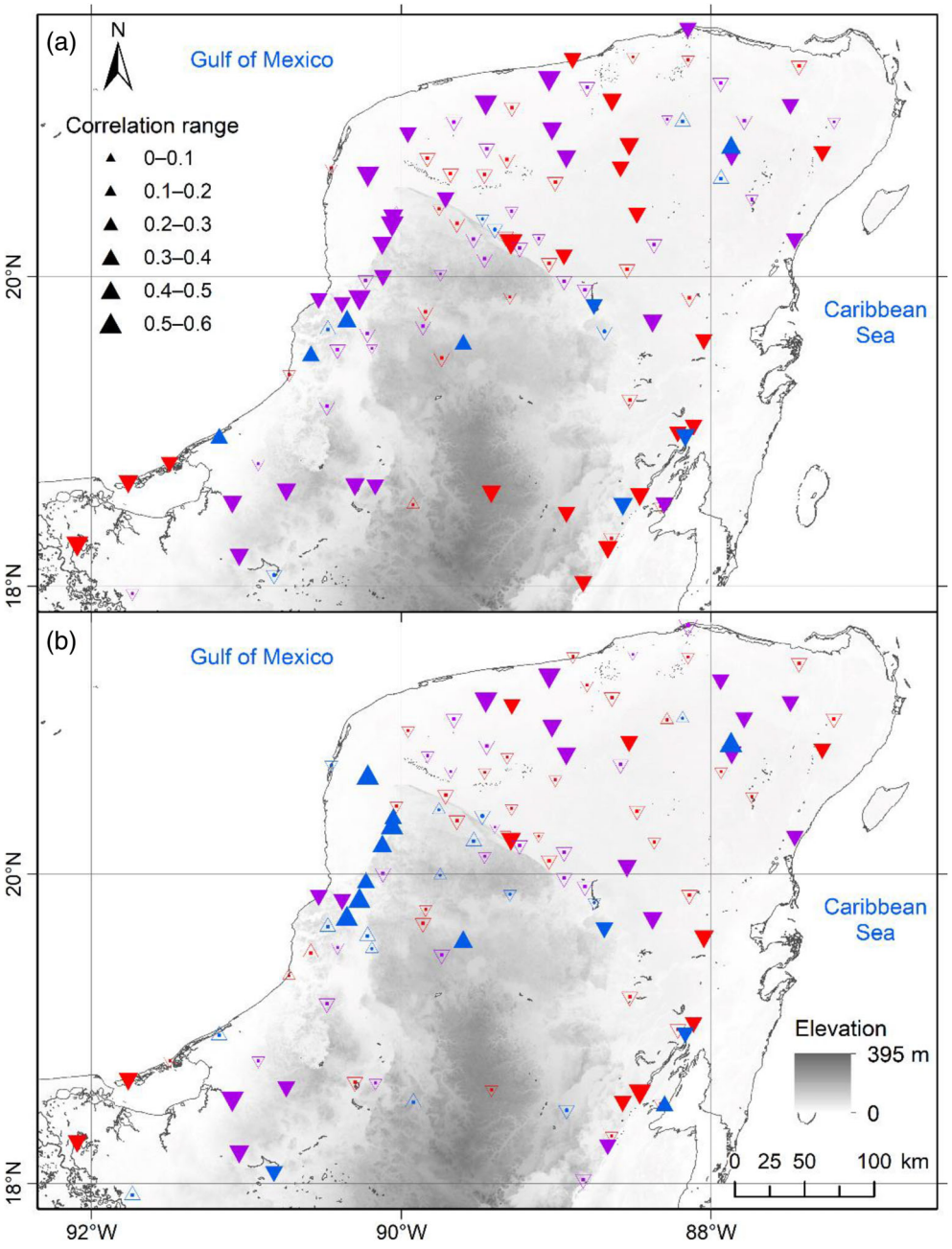

FIGURE 4 Spearman's correlation between climate indices and (a) rainy season accumulated precipitation and (b) dR20 variables. Blue triangles correspond to AMO; red, to NIÑO3.4; purple, to TII. Solid triangles represent correlations with a *p*-value ≤0.05, while non-solid triangles are for nonsignificative correlations. Triangles pointing up indicate positive, and inverted triangles designate negative correlations. [Colour figure can be viewed at wileyonlinelibrary.com]

None of the stations analysed showed a positive correlation with NIÑO3.4 or the TII. Some negative relationships with the AMO were observed, mainly for stations located in the centre and southeast of the study area, with low correlation values in general (Figure 4).

3.4 | RSAP analysis from gridded data

The analysis of CHIRPS gridded data showed a non-significant trend in most of the YP; however, positive trends were found mainly in the west and, to a lesser extent, in the north and northeast (Figure 5a). This trend in CHIRPS data is consistent with the one based on stations, implying that RSAP has increased from 1981 to 2022 (Figure 3d); for the YP stations, a positive but non-significant trend was also observed in the median of the RSAP from 1978 to 2020. Although large areas with significant trends yielded a positive relationship, a few negative trends were found in the southeast and extreme southwest.

Each index has an area of influence in the study area. RSAP showed a significant positive relationship with AMO in 26.9% of the territory and negative relationships with NIÑO3.4 and TII in 58.7% and 54.7% of the area, respectively. The zoning that led to obtaining these

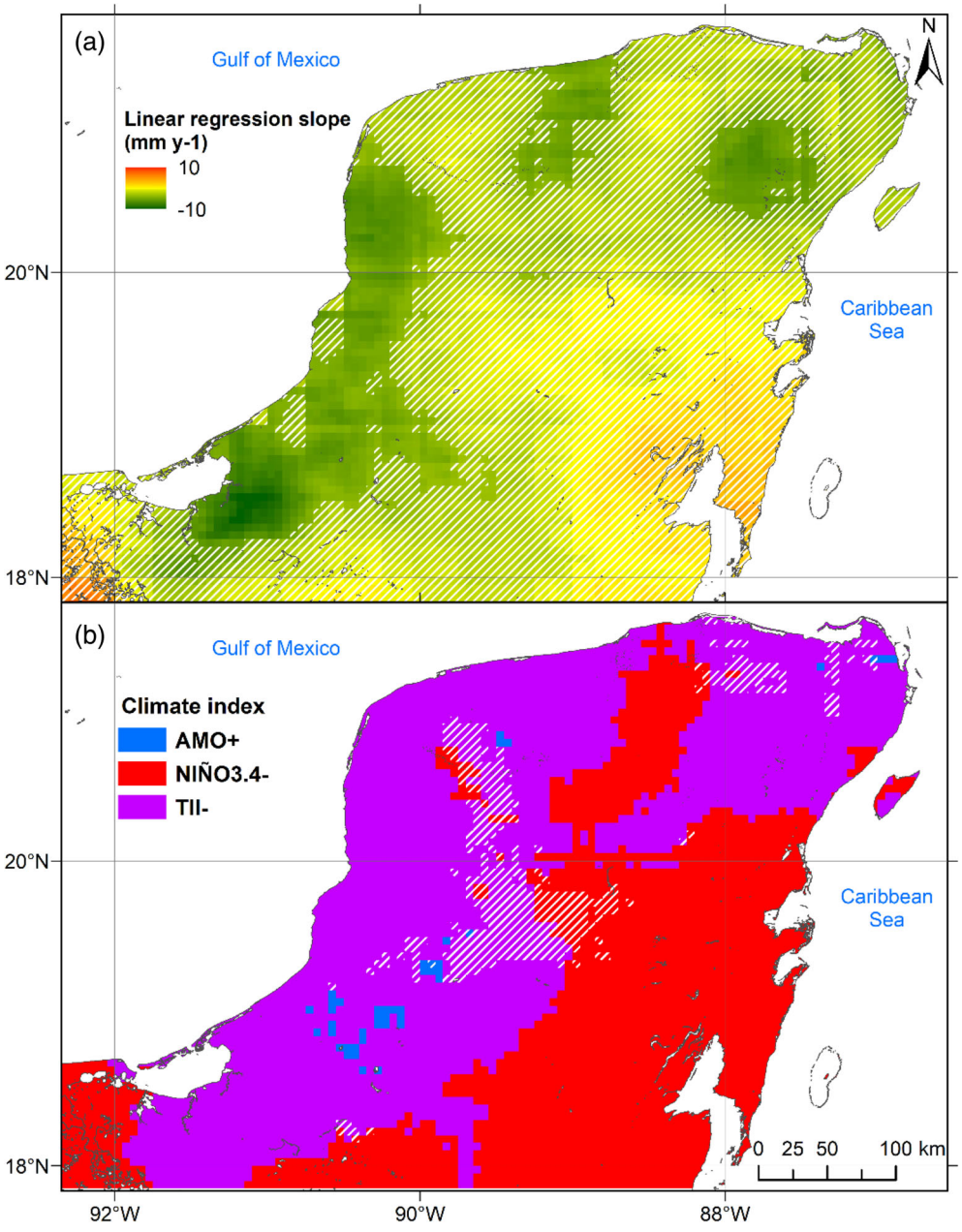

FIGURE 5 (a) Linear regression trends (mm·year^{-1}) and (b) climate index with the highest linear regression slope for the RSAP variable analysis calculated from CHIRPS. The sign + or − refers to the sign of the correlation. Areas with white hatching have *p*-values ≥0.05. [Colour figure can be viewed at wileyonlinelibrary.com]

percentages is presented in Figures S2–S4. Figure 5b is the equivalent of Figure 4a using CHIRPS data. A significant relationship with TII dominates the study region, particularly in the northeast, north and west of the YP, while NIÑO3.4 dominates most of the south and west. The areas with positive trends in Figure 5a correspond to sectors of TII dominance plus some others where AMO dominates. These findings confirm the relationships explained above related to Figure 4a. However, this methodology gives us better spatial coverage by leveraging the fact that the CHIRPS gridded data smooth out microclimatic aspects that may be present when gauge stations are used and provide continuous spatial and temporal data sets. However, the analysis through gauge stations is still highly relevant since the in situ observations allow validating data from CHIRPS grids.

Although we found significant positive trends and a relationship with the indices, it is worth considering that Shen et al. (2020) found that, in general, for large regions of the world, CHIRPS data showed a negative bias before 2000, attributed to infrared thermal satellite sensors. However, in the evaluations for Mesoamerica (Centella-Artola et al., 2020; Stewart et al., 2022), CHIRPS data yielded good validation results. No previous work was done specifically for the YP, but our results confirm the consistency between CHIRPS and gauged station data. To validate this consistency, we compared the signs of the Spearman correlation between station RSAP values and

climate indices with the linear regression estimates from CHIRPS. The sign of the relationship matched 87.5% and 97.8% of the stations with significant values. The non-matching results were the two negative relationships between RSAP and AMO (Table 1).

4 | DISCUSSION AND CONCLUSIONS

The YP rainy season shows significant spatial and inter-annual variations. This season is mainly dominated by a bimodal annual cycle, with maxima in June and September separated by a relative minimum around July–August called the Midsummer Drought (García-Franco et al., 2023; Perdigón-Morales et al., 2018). The main sources of moisture in the region are the tropical North Atlantic Ocean and the Caribbean Sea (Durán-Quesada et al., 2017). The rainy season lasts approximately four to 6 months, being shorter in the northwest than in the rest of the study area. Regarding the high temporal variability, in general, significant trends were found for the main characteristics of the rainy season, onset date, demise date, RSAP and dR20 but with a high spatial variation. The use of CHIRPS data allowed the identification of the main regions with statistically significant positive rainfall trends. These results are consistent with those reported by Mardero et al. (2020) for the south-centre of the YP. On the other hand, we observed a trend toward an increasing number of days of heavy rains (dR20) and a delay in the rainy season demise date, meaning a longer duration. The increase in dR20 could be associated with variation in convective systems, but also with easterly waves and tropical cyclones, for example, Romero and León-Cruz (2024) noticed a slight increase in tropical cyclone activity in the study area between 1950 and 2020. In addition to an increase in the number of days of heavy rains with a relatively stable total of days with lighter rain, we observed that the intraseasonal distribution of precipitation has changed to some extent. Note that these trends were calculated for periods of ~40 years only, so they should not be linked to climate change without a study supporting this relationship, as this region is influenced by known inter-annual and decadal climate sources of variability such as AMO and ENSO (Pascale et al., 2021). Although the long-term trends for the rainy season onset date or cumulative rainfall were significant for the study area as a whole, it is necessary to limit the degree to which certain conclusions can be drawn about the overall changes on the onset of the rainy season or the total amount of rainfall in a particular meteorological station. Furthermore, a limitation of the methodology used to determine the rainy season onset and demise dates is based on precipitation only and does not include evapotranspiration data (Hernández & Fernández, 2015) because very few stations have this type of data, and the time series are generally incomplete. For the demise date, there is also the issue of the gradual decrease in precipitation and the occurrence of cold fronts that do not allow the dates to be determined.

Another limitation is that the methods used are based on assumptions about climate variability and its impacts on local communities. These assumptions may not hold under changing climate conditions or for different regions. It is also critical to note that the variance associated with climate variability is greater than the long-term trend associated with climate change.

The main climatological characteristics of Mesoamerica throughout the evolution of the seasonal cycle have already been detailed by Martinez et al. (2019). Our results suggest that these characteristics are driven by SST variability in the equatorial eastern Pacific and the Atlantic oceans during the YP rainy season. The climate in the peninsula throughout the annual cycle is influenced by variations in the intra-American sea since the YP is surrounded by the Gulf of Mexico and the Caribbean Sea.

The variations observed in the oceanic indices suggest that humid conditions in the YP are generally favoured when relatively warmer-than-normal conditions occur in the Atlantic Ocean along with cold conditions in the eastern equatorial Pacific, especially during La Niña events. Wetter rainy seasons could be explained by a decrease in the strength of the Caribbean low-level jet stream (Amador, 2008; Hidalgo et al., 2015). This favours convection in the YP by reducing vertical wind shear and transferring humidity toward the overlying atmosphere from the surrounding seas due to increased latent heat transport (Amador et al., 2016). As the rainy season progresses, this behaviour is reinforced by the development of a warmer and more extended Western Hemisphere Warm Pool (Wang & Enfield, 2001, 2003). Additionally, during the AMO+ and NIÑO3.4− ocean configuration, tropical cyclone activity tends to increase (Martinez et al., 2023) in the Atlantic basin, which may contribute to more intense and even extreme rainfall events in the YP. Opposite conditions in these oceans favour relatively drier rainy seasons.

The results of Rodríguez Morales et al. (2023) for the coastal zone show the importance of AMO and ENSO as drivers of rainfall in the region. Our results are consistent with theirs in general terms, as AMO+ is related to more abundant rains in the north of the YP, while La Niña events in combination with AMO+ tend to be related to stronger rainy seasons.

An additional important aspect derived from our study is that the Atlantic and the eastern equatorial

Pacific should be compared only after the data are normalized because the AMO and NIÑO3.4 indices have different variances. The TII index developed in the present study incorporates this aspect by removing the influence of the central value (mean) and the variability (standard deviation) of SST data associated with the indices individually. TII explained most of the interannual variance of summer rains in a large portion of the YP.

Additionally, using grid data allowed us to expand the timeseries analysis to the entire YP to observe the relative spatial influence of the surrounding oceanic conditions and their interactions. However, these results should be validated through comparative analyses based on gauged stations.

The findings of the present study provide a better understanding of the climatic patterns in the YP region, which can be used to develop effective strategies for climate adaptation and risk management in different socioeconomic sectors. Indeed, the variation in precipitation during the rainy season is critical for key activities such as agriculture in tropical regions facing climate change (Hannah et al., 2017; Liu et al., 2021). The annual volume of rainfall exhibits a particularly marked interannual variation. This variability poses challenges for effective long-term planning and management of water resources, particularly in agricultural scenarios where a consistent rainfall pattern is imperative for successful crop cultivation.

AUTHOR CONTRIBUTIONS

David Romero: Conceptualization; methodology; software; data curation; investigation; validation; formal analysis; supervision; funding acquisition; visualization; project administration; resources; writing – original draft; writing – review and editing. **Eric J. Alfaro:** Conceptualization; methodology; software; data curation; investigation; writing – original draft; formal analysis; validation; writing – review and editing.

ACKNOWLEDGEMENTS

This research was funded by Programa de Apoyo a Proyectos de Investigación e Innovación Tecnológica (PAPIIT) of UNAM, grant number IA302220. EA thanks the following University of Costa Rica projects: C2806, C2103, A5-719, B9454 (supported by Fondo de Grupos), B0-810, A1-715, C3195, C0-130 and A4906 (PESCTMA).

DATA AVAILABILITY STATEMENT

The data that support the findings of this study are available in Trans-Isthmic-Index at https://github.com/dromeroRcode/Trans-Isthmic-Index. These data were derived from the following resources available in the public domain: David Romero, https://github.com/dromeroRcode/Trans-Isthmic-Index.

ORCID

David Romero https://orcid.org/0000-0002-1722-7514
Eric J. Alfaro https://orcid.org/0000-0001-9278-5017

REFERENCES

Abiy, A.Z., Melesse, A.M. & Abtew, W. (2019) Teleconnection of regional drought to ENSO, PDO, and AMO: southern Florida and the Everglades. *Atmosphere*, 10(6), 295. Available from: https://doi.org/10.3390/atmos10060295

Amador, J.A. (2008) The Intra-Americas sea low-level jet: overview and future research. *Annals of the New York Academy of Sciences*, 1146, 153–188. Available from: https://doi.org/10.1196/annals.1446.012

Amador, J.A., Durán-Quesada, A., Rivera, E., Mora, G., Sáenz, F., Calderón, B. et al. (2016) The easternmost tropical Pacific. Part II: seasonal and intraseasonal modes of atmospheric variability. *Revista de Biología Tropical*, 64, 23.

Andrade-Velázquez, M., Medrano-Pérez, O.R., Montero-Martínez, M.J. & Alcudia-Aguilar, A. (2021) Regional climate change in Southeast Mexico-Yucatan Peninsula, Central America and the Caribbean. *Applied Sciences*, 11(18), 8284. Available from: https://doi.org/10.3390/app11188284

Centella-Artola, A., Bezanilla-Morlot, A., Taylor, M.A., Herrera, D.A., Martinez-Castro, D., Gouirand, I. et al. (2020) Evaluation of sixteen gridded precipitation data sets over the Caribbean region using gauge observations. *Atmosphere*, 11(12), 1334. Available from: https://doi.org/10.3390/atmos11121334

Dunn, R.J., Alexander, L.V., Donat, M.G., Zhang, X., Bador, M., Herold, N. et al. (2020) Development of an updated global land in situ-based data set of temperature and precipitation extremes: HadEX3. *Journal of Geophysical Research: Atmospheres*, 125(16), e2019JD032263.

Dunning, C.M., Black, E. & Allan, R.P. (2018) Later wet seasons with more intense rainfall over Africa under future climate change. *Journal of Climate*, 31(23), 9719–9738. Available from: https://doi.org/10.1175/JCLI-D-18-0102.1

Durán-Quesada, A.M., Gimeno, L. & Amador, J. (2017) Role of moisture transport for Central American precipitation. *Earth System Dynamics*, 8(1), 147–161. Available from: https://doi.org/10.5194/esd-8-147-2017

Enfield, D.B. & Alfaro, E.J. (1999) The dependence of Caribbean rainfall on the interaction of the tropical Atlantic and Pacific oceans. *Journal of Climate*, 12(7), 2093–2103. Available from: https://doi.org/10.1175/1520-0442(1999)012<2093:TDOCRO>2.0.CO;2

Enfield, D.B., Mestas-Nuñez, A.M., Mayer, D.A. & Cid-Serrano, L. (1999) How ubiquitous is the dipole relationship in tropical Atlantic sea surface temperatures? *Journal of Geophysical Research: Oceans*, 104(C4), 7841–7848. Available from: https://doi.org/10.1029/1998JC900109

Enfield, D.B., Mestas-Nuñez, A.M. & Trimble, P.J. (2001) The Atlantic multidecadal oscillation and its relation to rainfall and river flows in the continental U.S. *Geophysical Research Letters*,

28(10), 2077–2080. Available from: https://doi.org/10.1029/2000GL012745

Funk, C., Peterson, P., Landsfeld, M., Pedreros, D., Verdin, J., Shukla, S. et al. (2015) The climate hazards infrared precipitation with stations—a new environmental record for monitoring extremes. *Scientific Data*, 2(1), 1–21.

García, E. (2004) *Modificaciones al sistema de clasificación climática de Köppen*. Ciudad de México, Mexico: Universidad Nacional Autónoma de México, Instituto de Geografía.

García-Franco, J.L., Chadwick, R., Gray, L.J., Osprey, S. & Adams, D.K. (2023) Revisiting mechanisms of the mesoamerican midsummer drought. *Climate Dynamics*, 60(1–2), 549–569. Available from: https://doi.org/10.1007/s00382-022-06338-6

García-García, D. & Ummenhofer, C.C. (2015) Multidecadal variability of the continental precipitation annual amplitude driven by AMO and ENSO: decadal precipitation driven by AMO/-ENSO. *Geophysical Research Letters*, 42(2), 526–535. Available from: https://doi.org/10.1002/2014GL062451

Goly, A. & Teegavarapu, R.S.V. (2014) Individual and coupled influences of AMO and ENSO on regional precipitation characteristics and extremes. *Water Resources Research*, 50(6), 4686–4709. Available from: https://doi.org/10.1002/2013WR014540

Gramzow, R.H. & Henry, W.K. (1972) The rainy pentads of Central America. *Journal of Applied Meteorology*, 11(4), 637–642. Available from: https://doi.org/10.1175/1520-0450(1972)011<0637:TRPOCA>2.0.CO;2

Hannah, L., Donatti, C.I., Harvey, C.A., Alfaro, E., Rodriguez, D.A., Bouroncle, C. et al. (2017) Regional modeling of climate change impacts on smallholder agriculture and ecosystems in Central America. *Climatic Change*, 141(1), 29–45. Available from: https://doi.org/10.1007/s10584-016-1867-y

Hernández, K. & Fernández, W. (2015) Estudio de la evaporación para el cálculo del inicio y la conclusión de la época seca y lluviosa en Costa Rica. *Tópicos Meteorológicos y Oceanográficos*, 14, 18–26.

Hidalgo, H.G., Durán-Quesada, A.M., Amador, J.A. & Alfaro, E.J. (2015) The caribbean low-level jet, the inter-tropical convergence zone and precipitation patterns in the intra-Americas Sea: a proposed dynamical mechanism. *Geografiska Annaler, Series A: Physical Geography*, 97(1), 41–59. Available from: https://doi.org/10.1111/geoa.12085

Hoerling, M., Eischeid, J. & Perlwitz, J. (2010) Regional precipitation trends: distinguishing natural variability from anthropogenic forcing. *Journal of Climate*, 23(8), 2131–2145. Available from: https://doi.org/10.1175/2009JCLI3420.1

INEGI. (2021) *Censo de Población y Vivienda 2020*. Aguascalientes, Mexico: Instituto Nacional de Estadística y Geografía. Available from: https://www.inegi.org.mx/programas/ccpv/2020/

IPCC. (2022) Summary for policymakers. In: *Climate change 2022: impacts, adaptation, and vulnerability. Contribution of working group II to the sixth assessment report of the Intergovernmental Panel on Climate Change*. Cambridge: Cambridge University Press, p. 34.

Karl, T.R., Nicholls, N. & Ghazi, A. (1999) Clivar/GCOS/WMO workshop on indices and indicators for climate extremes workshop summary. In: *Weather and climate extremes: changes, variations and a perspective from the insurance industry*. Dordrecht: Springer, pp. 3–7. https://doi.org/10.1007/97-8-9-4-01-5-926-5-_92

Kling, H., Fuchs, M. & Paulin, M. (2012) Runoff conditions in the upper Danube basin under an ensemble of climate change scenarios. *Journal of Hydrology*, 424–425, 264–277. Available from: https://doi.org/10.1016/j.jhydrol.2012.01.011

Kwon, M., Yeh, S., Park, Y. & Lee, Y. (2013) Changes in the linear relationship of ENSO–PDO under the global warming. *International Journal of Climatology*, 33(5), 1121–1128. Available from: https://doi.org/10.1002/joc.3497

Levine, A.F.Z., McPhaden, M.J. & Frierson, D.M.W. (2017) The impact of the AMO on multidecadal ENSO variability. *Geophysical Research Letters*, 44(8), 3877–3886. Available from: https://doi.org/10.1002/2017GL072524

Liu, L., Wang, X., Feng, G., Dogar, M.M., Zhang, F., Zhiqiang, G. et al. (2021) Variation of main rainy-season precipitation in eastern China and relevance to regional warming. *International Journal of Climatology*, 41(3), 1767–1783. Available from: https://doi.org/10.1002/joc.6929

Magaña, V.O., Amador, J.A. & Medina, S. (1999) The midsummer drought over Mexico and Central America. *Journal of Climate*, 12(6), 1577–1588.

Magaña, V.O. & Vázquez, J.L. (2000) *Interannual variability of northern activity over the Americas*. Reprints of the 24th conference on hurricanes and tropical meteorology, May 29–June 2, 2000.

Maldonado, T., Alfaro, E., Rutgersson, A. & Amador, J.A. (2017) The early rainy season in Central America: the role of the tropical North Atlantic SSTs. *International Journal of Climatology*, 37(9), 3731–3742. Available from: https://doi.org/10.1002/joc.4958

Maldonado, T., Rutgersson, A., Alfaro, E., Amador, J. & Claremar, B. (2016) Interannual variability of the midsummer drought in Central America and the connection with sea surface temperatures. *Advances in Geosciences*, 42, 35–50. Available from: https://doi.org/10.5194/adgeo-42-35-2016

Mardero, S., Schmook, B., Christman, Z., Metcalfe, S.E. & De La Barreda-Bautista, B. (2020) Recent disruptions in the timing and intensity of precipitation in Calakmul, Mexico. *Theoretical and Applied Climatology*, 140(1–2), 129–144. Available from: https://doi.org/10.1007/s00704-019-03068-4

Mardero, S., Schmook, B., López-Martínez, J., Cicero, L., Radel, C. & Christman, Z. (2018) The uneven influence of climate trends and agricultural policies on maize production in the Yucatan Peninsula, Mexico. *Land*, 7(3), 80. Available from: https://doi.org/10.3390/land7030080

Martinez, C., Goddard, L., Kushnir, Y. & Ting, M. (2019) Seasonal climatology and dynamical mechanisms of rainfall in the Caribbean. *Climate Dynamics*, 53(1–2), 825–846. Available from: https://doi.org/10.1007/s00382-019-04616-4

Martinez, L.-C., Romero, D. & Alfaro, E.J. (2023) Assessment of the spatial variation in the occurrence and intensity of major hurricanes in the Western Hemisphere. *Climate*, 11(1), 15. Available from: https://doi.org/10.3390/cli11010015

Martins, A. (2021) Cambio climático: los fenómenos adversos a los que se enfrentará América Latina, según el contundente informe de la ONU *BBC*, 13 August.

McGregor, G.R. & Nieuwolt, S. (1998) *Tropical climatology: an introduction to the climates of the low latitudes*. New York, NY: Wiley.

McKee, T.B., Doesken, N.J. & Kleist, J. (1993) The relationship of drought frequency and duration to time scales. In: *Proceedings of the 8th conference on applied climatology, Anaheim, California*. Boston, MA: American Meteorological Society, pp. 17–22.

Pascale, S., Kapnick, S.B., Delworth, T.L., Hidalgo, H.G. & Cooke, W.F. (2021) Natural variability vs forced signal in the 2015–2019 Central American drought. *Climatic Change*, 168(3–4), 16. Available from: https://doi.org/10.1007/s10584-021-03228-4

Pavia, E.G., Graef, F. & Reyes, J. (2006) PDO–ENSO effects in the climate of Mexico. *Journal of Climate*, 19(24), 6433–6438. Available from: https://doi.org/10.1175/JCLI4045.1

Penland, C. & Matrosova, L. (1998) Prediction of tropical Atlantic Sea surface temperatures using linear inverse modeling. *Journal of Climate*, 11(3), 483–496. Available from: https://doi.org/10.1175/1520-0442(1998)011<0483:POTASS>2.0.CO;2

Perdigón-Morales, J., Romero-Centeno, R., Pérez, P.O. & Barrett, B.S. (2018) The midsummer drought in Mexico: perspectives on duration and intensity from the CHIRPS precipitation database. *International Journal of Climatology*, 38(5), 2174–2186. Available from: https://doi.org/10.1002/joc.5322

Peterson, T., Folland, C., Gruza, G., Hogg, W., Mokssit, A. & Plummer, N. (2001) *Report on the activities of the working group on climate change detection and related rapporteurs*. Geneva: World Meteorological Organization.

Rodríguez Morales, U., Corona Vásquez, B., Prieto González, R. & Martínez, A.P. (2023) Influence of the AMO and its modulation of the ENSO effects on summer precipitation in Mexican coastal regions. *Water Practice and Technology*, 18(2), 304–319. Available from: https://doi.org/10.2166/wpt.2023.015

Romero, D., Alfaro, E., Orellana, R. & Hernandez Cerda, M.-E. (2020) Standardized drought indices for pre-summer drought assessment in tropical areas. *Atmosphere*, 11(11), 1209. Available from: https://doi.org/10.3390/atmos11111209

Romero, D. & León-Cruz, J.F. (2024) Spatiotemporal changes in hurricane-force wind risk assessment in the Yucatan Peninsula, Mexico. *Natural Hazards*, 120, 4675–4698. Available from: https://doi.org/10.1007/s11069-023-06397-w

Romero, D., Torres-Irineo, E., Kern, S., Orellana, R. & Hernandez-Cerda, M.E. (2017) Determination of the soil moisture recession constant from satellite data: a case study of the Yucatan Peninsula. *International Journal of Remote Sensing*, 38(20), 5793–5813. Available from: https://doi.org/10.1080/01431161.2017.1346844

Sáenz, F., Hidalgo, H.G., Muñoz, Á.G., Alfaro, E.J., Amador, J.A. & Vázquez-Aguirre, J.L. (2023) Atmospheric circulation types controlling rainfall in the Central American isthmus. *International Journal of Climatology*, 43(1), 197–218. Available from: https://doi.org/10.1002/joc.7745

Shen, Z., Yong, B., Gourley, J.J., Qi, W., Lu, D., Liu, J. et al. (2020) Recent global performance of the climate hazards group infrared precipitation (CHIRP) with stations (CHIRPS). *Journal of Hydrology*, 591, 125284. Available from: https://doi.org/10.1016/j.jhydrol.2020.125284

SIAP. (2021) *Datos abiertos—estadística de producción agrícola*. Ciudad de México, Mexico: Servicio de Información Agroalimentaria y Pesquera.

Soley, F. (1994) Suavizamiento de series cronológicas geofísicas con ruido blanco y rojo aditivo. *Revista Geofisica*, 41(1), 33–58.

Stewart, I.T., Maurer, E.P., Stahl, K. & Joseph, K. (2022) Recent evidence for warmer and drier growing seasons in climate sensitive regions of Central America from multiple global data sets. *International Journal of Climatology*, 42(3), 1399–1417. Available from: https://doi.org/10.1002/joc.7310

Toshie Kayano, M. & Buscioli, C.V. (2014) How the Atlantic multidecadal oscillation (AMO) modifies the ENSO influence on the South American rainfall. *International Journal of Climatology*, 34(1), 162–178. Available from: https://doi.org/10.1002/joc.3674

Trenberth, K.E. & Stepaniak, D.P. (2001) Indices of El Niño evolution. *Journal of Climate*, 14(8), 1697–1701. Available from: https://doi.org/10.1175/1520-0442(2001)014<1697:LIOENO>2.0.CO;2

Vidal, R. (2005) *Las regiones climáticas de México*. Mexico: Instituto de Geografía UNAM.

Wang, C. (2019) Three-ocean interactions and climate variability: a review and perspective. *Climate Dynamics*, 53(7–8), 5119–5136. Available from: https://doi.org/10.1007/s00382-019-04930-x

Wang, C. & Enfield, D.B. (2001) The tropical Western Hemisphere warm pool. *Geophysical Research Letters*, 28(8), 1635–1638. Available from: https://doi.org/10.1029/2000GL011763

Wang, C. & Enfield, D.B. (2003) A further study of the tropical Western Hemisphere warm pool. *Journal of Climate*, 16, 1476–1493. Available from: https://doi.org/10.1175/1520-0442(2003)016<1476:AFSOTT>2.0.CO;2

Wilks, D.S. (2019) *Statistical methods in the atmospheric sciences*. Amsterdam and Cambridge, MA: Elsevier.

WMO. (2017) *WMO guidelines on the calculation of climate normals*. Geneva: WMO.

Zárate-Hernández, E. (2013) Climatología de masas invernales de aire frío que alcanzan Centroamérica y el Caribe y su relación con algunos índices Árticos. *Tópicos Meteorológicos y Oceanográficos*, 12(1), 35–55.

SUPPORTING INFORMATION

Additional supporting information can be found online in the Supporting Information section at the end of this article.

How to cite this article: Romero, D., & Alfaro, E. J. (2024). Spatiotemporal variability of the rainy season in the Yucatan Peninsula. *International Journal of Climatology*, 1–14. https://doi.org/10.1002/joc.8468